Biochemical and Biophysical Research Communications 412 (2011) 155–159

Contents lists available at ScienceDirect

Biochemical and Biophysical Research Communications

journal homepage: www.elsevier.com/locate/ybbrc

Enhanced dynamic range in a genetically encoded Ca^{2+} sensor

Shun Liu [a,b,1], Jun He [c,1], Honglin Jin [a,b], Fei Yang [a,b], Jinling Lu [a,b], Jie Yang [a,b,*]

[a] Britton Chance Center for Biomedical Photonics, Wuhan National Laboratory for Optoelectronics-Huazhong University of Science and Technology, Wuhan 430074, China
[b] Key Laboratory of Biomedical Photonics of Ministry of Education, Huazhong University of Science and Technology, Wuhan 430074, China
[c] Division of Histology and Embryology, Tongji Medical College, Huazhong University of Science and Technology, Wuhan 430030, China

ARTICLE INFO

Article history:
Received 11 July 2011
Available online 22 July 2011

Keywords:
FRET (Fluorescent Resonant Energy Transfer)
Biosensor
Dynamic range

ABSTRACT

Genetically encoded fluorescence resonance energy transfer (FRET) indicators are powerful tools for real-time detection of second messenger molecules and activation of signal proteins. However, these fluorescent protein-based sensors typically display marginal FRET efficiency. To improve their FRET efficiency for optical imaging and screening, we developed a number of fluorescent protein mutants based on cyan fluorescent protein (CFP) and yellow fluorescent protein (YFP). To improve FRET ratios, which were initially within a narrow dynamic range, we used DNA shuffling to develop a new FRET pair called 3xCFP/Venus. The optimized 3xCFP/Venus pair exhibited higher FRET ratios than CyPet/YPet, which has one of the greatest dynamic ranges of protein-based FRET pairs. We converted this FRET pair to a Ca^{2+} FRET indicators using circular permutation Venus (cpVenus) linked with 3xCFP to form 3xCFP/cpVenus, which displayed an ~11-fold change in dynamic range in response to Ca^{2+} binding. The enhanced dynamic range for Ca^{2+} concentration detection using 3xCFP/cpVenus was confirmed in PC12 cells using previously established indicators (TN-XXL, ECFP/cpCitrine). To our knowledge, this FRET pair displays the largest dynamic range so far among genetically-encoded sensors, and can be used for sensitive FRET detection.

1. Introduction

Fluorescence resonance energy transfer (FRET) is a powerful tool to detect dynamic cellular events, such as protein–protein interactions and protein conformational changes [1–3]. For studies in living cells, cyan (CFP) and yellow (YFP) fluorescent protein (FP) are the most common genetically-encoded FRET pair and can be designed as indicators to study intracellular biochemical reaction processes. Generally, there are two types of FP-based intra-molecular FRET indicators: reversible and irreversible [4]. The reversible indicators have been used to detect ion concentration and kinase activity, while the irreversible indicators have mainly been used to examine proteinase activity, such as that of caspases [5] and MMPs [6]. In theory, an ideal FRET pair should be suitable for both reversible and irreversible applications. Moreover, for a FRET indicator to be efficient, it must have sufficient dynamic range to guarantee sensitive detection of fluorescent signal fluctuations. However, FRET signals often exhibit limited dynamic range and sensitivity using reported FPs, such as CFP series (ECFP and Cerulean [7]) and YFP series (EYFP and Citrine [8]). Recently, a FRET pair of CyPet/YPet, which was screened using fluorescence-activated cell sorting, improved dynamic range, providing a sevenfold enhancement of the FRET signal when used as an irreversible caspase indicator [9]. However, CyPet/YPet might not be an ideal reversible indicator, due to hydrophobic substitutions on the S208F and V224L residues of their barrel structure surfaces, resulting in intramolecular complex formation, which makes CyPet and YPet difficult to separate [9]. Thus, the dynamic range of response was limited when the CyPet/YPet was used as a reversible FRET reporter.

As one of the most popular reversible indicators, calcium FRET sensors, are widely applied in the measurement of calcium ion concentration changes in living cells. To detect these changes, many versions of genetically encoded FRET calcium sensors using CFP/YFP derivatives have been developed based on the calcium ion binding proteins calmodulin (CaM) [10–14] or troponin C (TnC) [15–18], sandwiched between CFP and YFP as a calcium-binding domain. When these FRET calcium indicators bind Ca^{2+}, the calcium-binding domain changes its structural conformation and consequently alters both the orientation and distance between the CFP and YFP, resulting in a ratiometric change in emission intensities. Although current FRET indicators, such as YC3.6 [21], TN-XXL [18], have shown a 5–6-fold change in dynamic range, further studies are required to improve dynamic ranges to achieve more sensitive detection of Ca^{2+} alterations in living cells. To improve reversible FRET sensor dynamic range for detection of Ca^{2+},

* Corresponding author at: Key Laboratory of Biomedical Photonics of Ministry of Education, Huazhong University of Science and Technology, Wuhan 430074, China. Fax: +86 27 8779 2034.
E-mail address: yangjie@mail.hust.edu.cn (J. Yang).
[1] These authors contributed equally to this work.

0006-291X/$ - see front matter © 2011 Elsevier Inc. All rights reserved.
doi:10.1016/j.bbrc.2011.07.065

we used an alternative approach to screen for an optimum FRET CFP donor by using DNA shuffling, which is a rapid method to direct large-scale DNA libraries by propagating beneficial mutations. The objective of this study was to take advantage of the selected CFP variant to pair with various FP acceptors in the aim of obtaining an optimum FRET indicator that could serve as both reversible and irreversible FRET sensors.

2. Materials and methods

2.1. Mutagenesis and construction

To construct novel variants of fluorescent proteins, we used the StEP method, a DNA shuffling mutation technique [19], to mutate the cyan fluorescent protein genes. The genes of Cerulean, EYFP, mCitrine, ECFP, EGFP, Venus were mixed as shuffling mutation templates. The cDNAs were cloned into *BamH*I–*Hind*III sites in the plasmid pRSETb. The plasmids were transformed into competent *Escherichia coli* DH5α and grown overnight on Luria–Bertani (LB)/agar plates containing 50 μg/ml ampicillin at 37 °C.

The cDNA of TN-XXL (ECFP–TN–cpCitrine) was provided by Dr. Oliver Griesbeck [18]. We replaced ECFP/cpCitrine pair with 3xCFP/cpVenus, 3xCFP/cpCitrine, CyPet/YPet and 3xCFP/Venus pairs. To construct the vectors for mammalian cells, a Kozak sequence (GCCACCATGG) was introduced into the plasmid. The cDNA probes were cloned into pcDNA3.1 (Invitrogen) with *BamH*I/*EcoR*I restriction sites.

2.2. Protein expression, in vitro spectroscopy and titrations

All recombinant proteins with a 6His-tag were expressed in *E. coli* BL21 (DE3) and induced by 0.5 mM IPTG at room temperature overnight. Proteins were purified with Ni–NTA His SpinTrap™. Spectral measurement was performed by a spectrofluorometer (FP-6500, Jasco). The calcium-free buffer consisted of 25 μM EGTA in 100 mM KCl and 10 mM MOPS, pH 7.5 and the calcium-activated buffer consisted of 10 mM $CaCl_2$ in 100 mM KCl and 10 mM MOPS, pH 7.5. The calcium titration was performed according to the protocol of calcium calibration kit (Invitrogen). Fluorescence emission spectra were between 450 and 600 nm with 433-nm excitation. The ratio was calculated according to the maximum emission peaks of the donor and acceptor. The concentrations of purified fluorescent proteins were measured using a BCA Assay Kit (Shanghai Sangon Corp.).

2.3. Ca^{2+} imaging

A dual channel imaging approach was used to collect CFP and FRET images using an Olympus FV500 confocal microscope. A 405-nm diode laser light source was used and dual channel fluorescence emission channels were recorded simultaneously. The emission fluorescence was acquired in the ranges 450–510 nm (CFP channel) and 540–625 nm (FRET channel) using a 20× objective lens. The FRET ratio was calculated as formula: R = Intensity of FRET/Intensity of acceptor. The dynamic range was calculated as formula: $\Delta R/R_0 = (R_{max}-R_0)/R_0$, where R_0 stands for the initial ratio and R_{max} stands for maximal ratio. Images were analyzed using Fluoview imaging software (Olympus, Tokyo) and Image J.

3. Results

3.1. Developing a new CFP variant 3xCFP as a FRET donor

To improve the FRET efficiency, we constructed a mutant library for screening an optimum FRET donor through DNA shuffling. From approximate 10^5 clones, a variant with the mutation sites (ECFP S72A/I146N/T153M/S175G), named 3xCFP, was identified due to its red-shift. The 3xCFP had an excitation peak at 442 nm and an emission peak at 482 nm (Fig. 1A), which increases spectral overlap with YFP excitation, which should enhance FRET efficiency. Next, we constructed a series of FRET pairs, including two previous reported the YPet/CyPet [9] and YPet/ECFP [20] pairs, linked by a short linker (sequence: LEVDVADGGSKDP) to assess the FRET efficiency. The spectral data showed that FRET ratios of YPet–13aa–CyPet and YPet–13aa–ECFP were 5.3 and 3.1, respectively (Fig. 1B). Under the same condition, the ratios of Venus–13aa–3xCFP and YPet–13aa–3xCFP were 8.4 and 3.2, respectively (Fig. 1B). Thus, 3xCFP/Venus had the greatest FRET efficiency among these FRET pairs, and these data suggested a critical role of 3xCFP in the enhancement of FRET efficiency, when paired with Venus.

3.2. Comparison of the dynamic ranges of different FRET pairs in vitro

To use 3xCFP and Venus as a reversible Ca^{2+} FRET indicator, we compared two constructed Ca^{2+} indicators, the 3xCFP/Venus pair and the CyPet/YPet pair; both sandwiched by the Ca^{2+} binding domain TnC. As shown in Table 1, the FRET/donor ratio of 3xCFP/Venus pair changed from 1.46 (no Ca^{2+}) to 2.77 (Ca^{2+} saturation), resulting

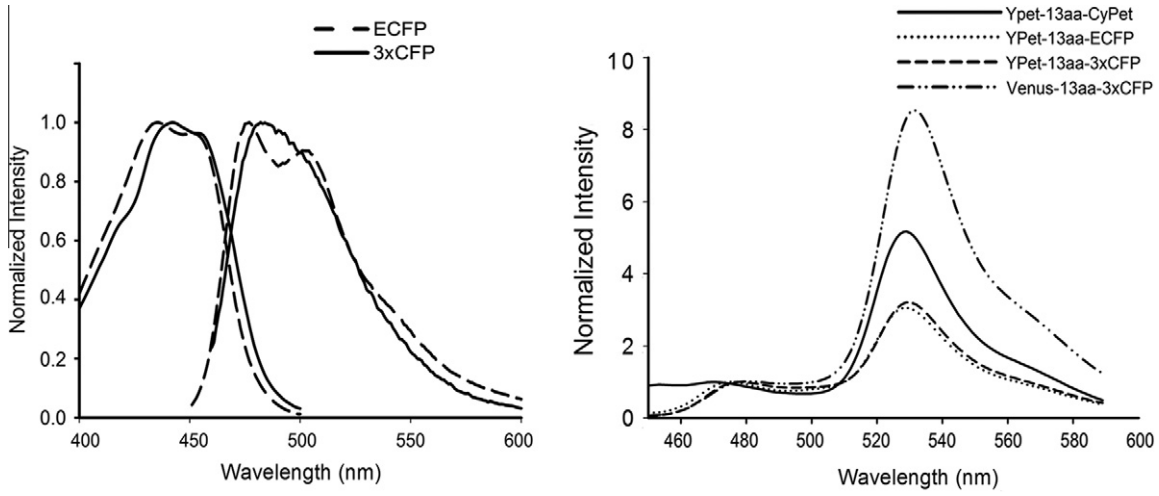

Fig. 1. Screening CFP variants as a FRET donor. (A) The excitation and emission spectra of ECFP (dashed line) and 3xCFP (solid line). (B) The FRET spectra of YPet–13aa–CyPet, YPet–13aa–ECFP, YPet–13aa–3xCFP and Venus–13aa–3xCFP.

Table 1
Effects of donor and acceptor replacements on free and saturated Ca^{2+}-induced changes in FRET ratios. The table shows the $\Delta R/R_0$ of the indicated FRET pairs (average values come from three repeats).

Donor–TnC–Acceptor	Free Ca^{2+}	Saturated Ca^{2+}	$\Delta R/R_0$ (%)
3xCFP–TnC–Venus	1.46	2.77	90
CyPet–TnC–YPet	1.73	3.49	102
CyPet–TnC–cpYPet	2.02	5.18	156
3xCFP–TnC–cpVenus	1.80	22.77	1165
TN-XXL (ECFP–TnC–cpCitrine)	0.95	5.80	510
3xCFP–TnC–cpCitrine	1.63	10.17	524

in a dynamic range of 99%. A similar ratio was obtained for CyPet/YPet, which changed from 1.73 (free Ca^{2+}) to 3.49 (Ca^{2+} saturation) with a ratiometric change of 102% (Table 1). These data demonstrated that both 3xCFP/Venus and CyPet/YPet pairs had relatively poor dynamic ranges, possibly due to unfavorable dipole alignment. It has been reported that the dynamic range of CyPet/YPet pair cannot readily be further improved, even if an optimum dipole angle is incorporated [16], because of the dimerizational interaction between S208F and V224L. Our result also demonstrated that CyPet–TnC–cpYPet had only a 156% dynamic range change (Table 1). To address this problem, we constructed a Ca^{2+} indicator 3xCFP–TnC–cpVenus, in which cpVenus (circular permutation Venus) was selected to alter the orientation of the chromophore for Ca^{2+} indicators [21]. After the successful construction of 3xCFP–TnC–cpVenus and its expression in *E. coli*, the 3xCFP–TnC–cpVenus protein was purified. Ca^{2+} titration showed that the FRET ratio of 3xCFP–TnC–cpVenus reached 22.77 when Ca^{2+} was saturated, and the ratio was 1.80 when Ca^{2+} was absent (Fig. 2B). Hence, the dynamic range of 3xCFP–TnC–cpVenus was 1165% (Table 1), which represents the largest dynamic range of FP FRET Ca^{2+} indicators so far. In comparison, the dynamic ranges of ECFP–TnC–cpCitrine (TN-XXL, a reported Ca^{2+} indicator with high dynamic range) and 3xCFP–TnC–cpCitrine were 510% and 524%, respectively (Table 1). We plotted calcium titration curves of 3xCFP–TnC–cpVenus and ECFP–TnC–cpCitrine to compare the calcium responses. The titration results showed that 3xCFP–TnC–cpVenus had a larger dynamic range than TN-XXL (Fig. 2B). Together, these data demonstrated that 3xCFP/cpVenus pair greatly expands the dynamic range for reversible Ca^{2+} FRET detection *in vitro*.

3.3. Calcium Imaging in PC12 Cells

To further confirm the enhanced dynamic range of 3xCFP–TnC–cpVenus in living cells, we made use of calcium store-operated channels (SOCs), which are located in the plasma membrane of non-excitable cells. SOCs are considered the major source of intracellular calcium [22] and are essential for cellular calcium homeostasis. To detect calcium changes, an experiment was performed in PC12 cells expressing 3xCFP–TnC–cpVenus and TN-XXL. Intracellular Ca^{2+} stores were first depleted by treating cells with the SERCA pump inhibitor thapsigargin (TG) in Ca^{2+}-free condition. Then, 2 mM extracellular Ca^{2+} was added into the medium to detect the SOC Ca^{2+} influx. As shown in Fig. 3B, the CFP (cyan lines) and FRET signal (yellow lines) of 3xCFP–TnC–cpVenus experienced dramatic changes with a concomitant extracellular Ca^{2+} influx. However, relatively small changes were observed for the CFP and FRET signal of TN-XXL (Fig. 3A). For a better comparison, we plotted the $\Delta R/R_0$ curves for cells of interest (Fig. 3C). The maximum average $\Delta R/R_0$ value of 3xCFP–TnC–cpVenus was much greater than TN-XXL, which were 1.86 ± 0.28 ($n = 5$ cells) and 0.68 ± 0.12 ($n = 5$ cells),

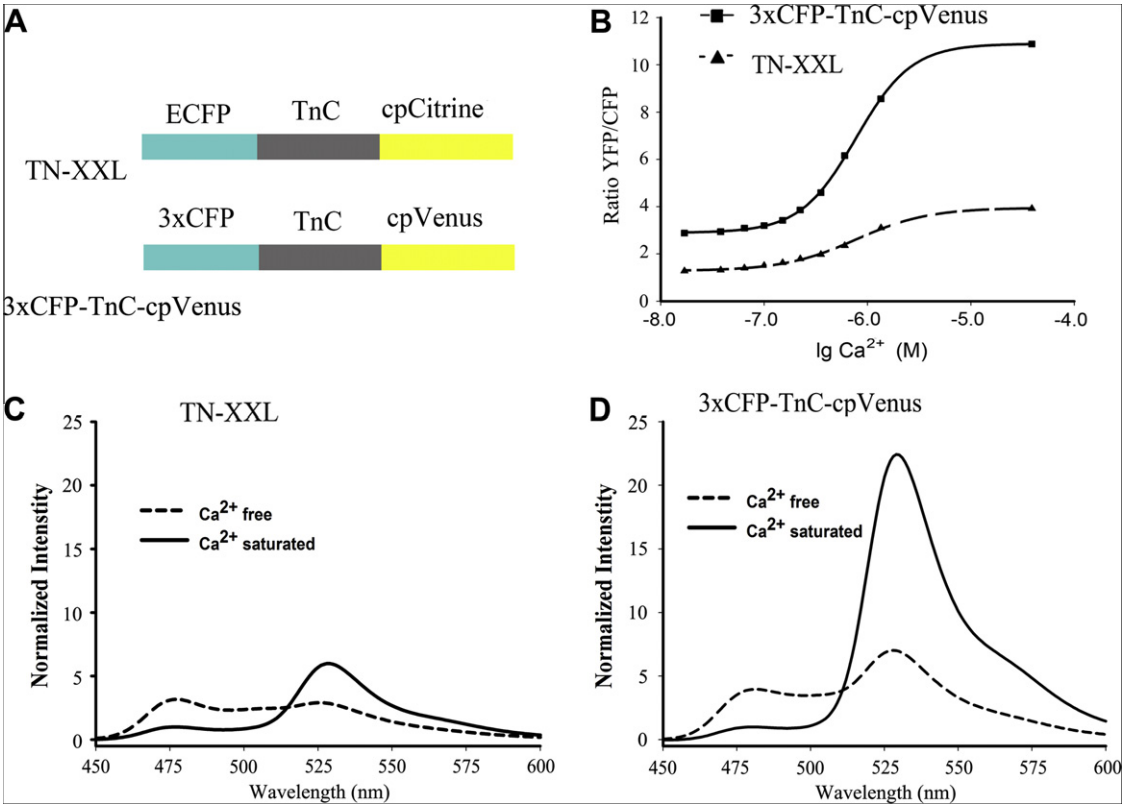

Fig. 2. Characterization of two Ca^{2+} indicators. (A) Schematic diagram of the construction of TN-XXL and 3xCFP–Tnc–cpVenus. (B) Ca^{2+} titration of the recombinant ECFP–TnC–cpCitrine (triangle) and 3xCFP–TnC–cpVenus (quadrangle) variants. The recombinant proteins were mixed with various concentrations of Ca^{2+}, and the YFP/CFP emission intensity ratios were measured and plotted as a function of log [Ca^{2+}]. (C) Ca^{2+} indicator ECFP–TnC–cpCitrine (TN-XXL) in Ca^{2+}-saturated (solid curves) and Ca^{2+}-free (dotted curves) buffer. (D) Ca^{2+} indicator 3xCFP–TnC–cpVenus in Ca^{2+}-saturated (solid curves) and Ca^{2+}-free (dotted curves) buffer.

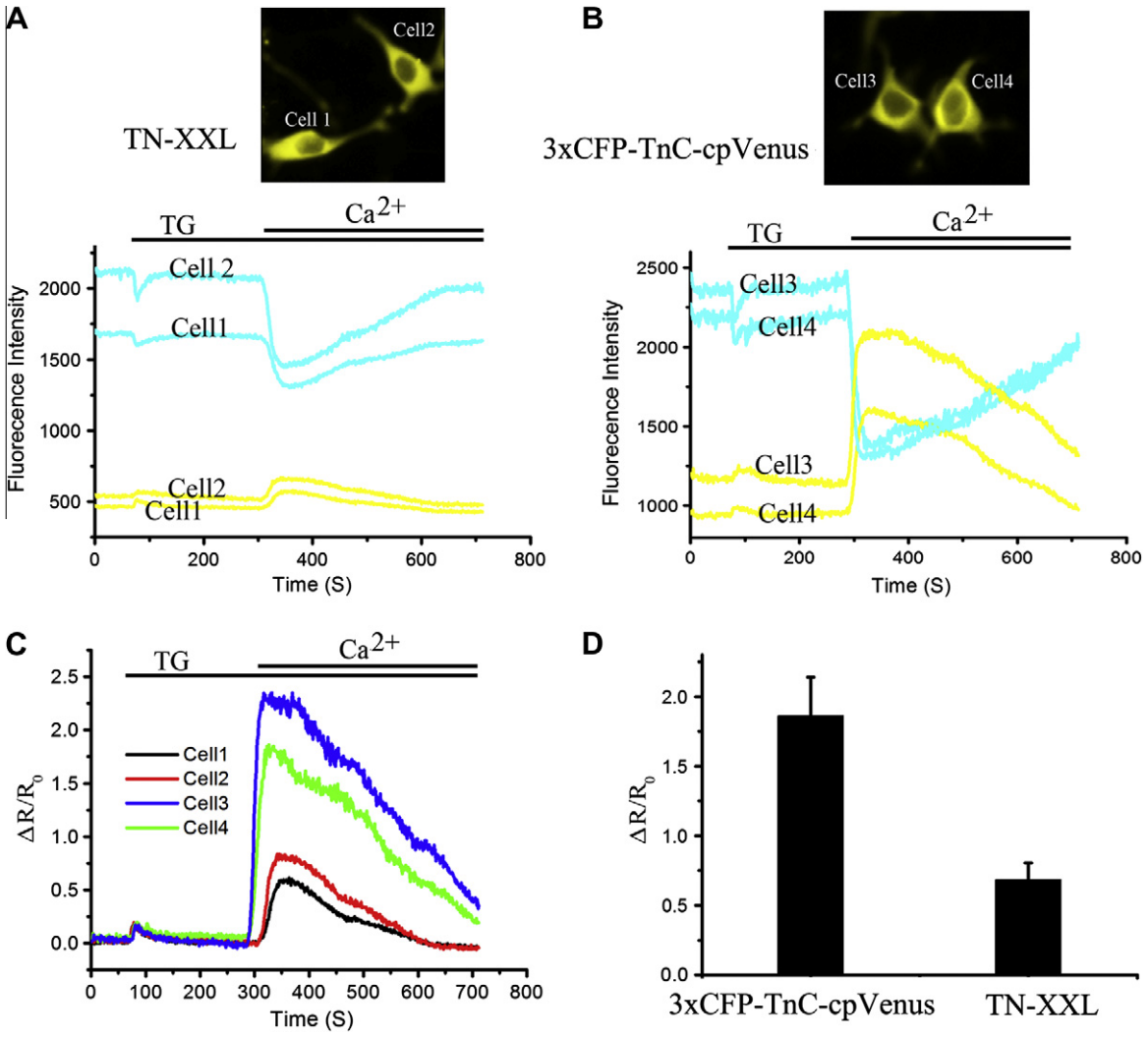

Fig. 3. Imaging of calcium SOCs in PC12 cells. (A) TN-XXL was expressed in PC12 cells. Cells were treated with the SERCA pump inhibitor thapsigargin (TG), followed by addition of 2 mM extracellular Ca^{2+}. The fluorescent intensities of cell1 and cell2 were recorded in dual channels of 450–510 nm (CFP channel) and 540–625 nm (FRET channel). (B) 3xCFP–TnC–cpVenus was expressed in PC12 cells which were also activated by TG. The fluorescent response signals of cell3 and cell4 in the CFP (cyan lines) and FRET (yellow lines) channel were obtained at the same time. (C) The $\Delta R/R_0$ change curves of cell 1, 2, 3, and 4 were plotted. (D) Comparison of TN-XXL and 3xCFP–TnC–cpVenus peak responses; the $\Delta R/R_0$ average values of 3xCFP–TnC–cpVenus and TN-XXL are 1.86 ± 0.28 ($n = 5$ cells) and 0.68 ± 0.12 ($n = 5$ cells), respectively. (For interpretation of the references to color in this figure legend, the reader is referred to the web version of this article.)

respectively (Fig. 3D). These data show that 3xCFP–TnC–cpVenus exhibited higher sensitivity than TN-XXL in PC12 cells.

4. Discussion

We developed a 3xCFP variant as a FRET donor for Venus, and this FRET pair exhibited a remarkably large FRET dynamic range. As a calcium indicator, 3xCFP was paired with cpVenus and exhibited approximately an 11-fold FRET ratio change in *in vitro*. Using a SOC model in PC12 cells, an approximate three fold improvement in dynamic range was obtained for 3xCFP–TnC–cpVenus compared with TN-XXL.

The emission spectrum of 3xCFP has enhanced overlap with the excitation spectrum of YFP acceptors and this led to the larger dynamic range. Interestingly, a further enhanced dynamic range was observed when 3xCFP paired with Venus or cpVenus. This may have been because Venus has certain mutation points that may increase the dimerization interface with 3xCFP, similar as the CyPet/YPet pair. Other factors, such as the basal FRET signal may also contribute to this process. 3xCFP/Venus or 3xCFP/cpVenus had large dynamic ranges, unlike CyPet/YPet pair with a high basal FRET signal. These results suggest that the interaction strength between 3xCFP and Venus was much weaker than that of CyPet/YPet pair. Therefore, it was easier to separate 3xCFP/Venus pair, which had a relative lower basal FRET ratio. Using the improved pair to design FRET indicators, the dynamic range was enhanced. Other applications using 3xCFP/Venus pair as a FRET indicator are currently under investigation. In summary, we developed a valuable FRET sensor 3xCFP/Venus with large FRET dynamic range, allowing sensitive and efficient calcium concentration measurements.

Acknowledgment

We thank Dr. Oliver Griesbeck for providing the TN-XXL plasmid, Dr. David Piston for pmCerulean-C1, and Dr. Atsushi Miyawaki for YC3.6. We also thank the Analytical and Testing Center, Huazhong University of Science and Technology, for the spectra measurements. This work was supported by the National Natural Science Foundation of China (Grant Nos. 30800208 and 30800339).

References

[1] U.B. Choi, P. Strop, M. Vrljic, S. Chu, A.T. Brunger, K.R. Weninger, Single-molecule FRET-derived model of the synaptotagmin 1-SNARE fusion complex, Nat. Struct. Mol. Biol. 17 (3) (2010) 318–324.

[2] K. Park, L.H. Lee, Y.B. Shin, S.Y. Yi, Y.W. Kang, D.E. Sok, J.W. Chung, B.H. Chung, M. Kim, Detection of conformationally changed MBP using intramolecular FRET, Biochem. Biophys. Res. Commun. 388 (3) (2009) 560–564.

[3] J. Bossuyt, S. Despa, F. Han, Z. Hou, S.L. Robia, J.B. Lingrel, D.M. Bers, Isoform specificity of the Na/K-ATPase association and regulation by phospholemman, J. Biol. Chem. 284 (39) (2009) 26749–26757.

[4] I. Kotera, T. Iwasaki, H. Imamura, H. Noji, T. Nagai, Reversible dimerization of Aequorea victoria fluorescent proteins increases the dynamic range of FRET-based indicators, ACS Chem. Biol. 5 (2) (2010) 215–222.

[5] H.W. Ai, K.L. Hazelwood, M.W. Davidson, R.E. Campbell, Fluorescent protein FRET pairs for ratiometric imaging of dual biosensors, Nat. Methods 5 (5) (2008) 401–403.

[6] J. Yang, Z. Zhang, J. Lin, J. Lu, B.F. Liu, S. Zeng, Q. Luo, Detection of MMP activity in living cells by a genetically encoded surface-displayed FRET sensor, Biochim. Biophys. Acta 1773 (3) (2007) 400–407.

[7] M.A. Rizzo, G.H. Springer, B. Granada, D.W. Piston, An improved cyan fluorescent protein variant useful for FRET, Nat. Biotechnol. 22 (4) (2004) 445–449.

[8] O. Griesbeck, G.S. Baird, R.E. Campbell, D.A. Zacharias, R.Y. Tsien, Reducing the environmental sensitivity of yellow fluorescent protein. Mechanism and applications, J. Biol. Chem. 276 (31) (2001) 29188–29194.

[9] A.W. Nguyen, P.S. Daugherty, Evolutionary optimization of fluorescent proteins for intracellular FRET, Nat. Biotechnol. 23 (3) (2005) 355–360.

[10] A. Miyawaki, J. Llopis, R. Heim, J.M. McCaffery, J.A. Adams, M. Ikura, R.Y. Tsien, Fluorescent indicators for Ca^{2+} based on green fluorescent proteins and calmodulin, Nature 388 (6645) (1997) 882–887.

[11] L. Tian, S.A. Hires, T. Mao, D. Huber, M.E. Chiappe, S.H. Chalasani, L. Petreanu, J. Akerboom, S.A. McKinney, E.R. Schreiter, C.I. Bargmann, V. Jayaraman, K. Svoboda, L.L. Looger, Imaging neural activity in worms, flies and mice with improved GCaMP calcium indicators, Nat. Methods 6 (12) (2009) 875–881.

[12] K. Truong, A. Sawano, H. Mizuno, H. Hama, K.I. Tong, T.K. Mal, A. Miyawaki, M. Ikura, FRET-based in vivo Ca^{2+} imaging by a new calmodulin-GFP fusion molecule, Nat. Struct. Biol. 8 (12) (2001) 1069–1073.

[13] J. Nakai, M. Ohkura, K. Imoto, A high signal-to-noise Ca^{2+} probe composed of a single green fluorescent protein, Nat. Biotechnol. 19 (2) (2001) 137–141.

[14] A.E. Palmer, M. Giacomello, T. Kortemme, S.A. Hires, V. Lev-Ram, D. Baker, R.Y. Tsien, Ca^{2+} indicators based on computationally redesigned calmodulin–peptide pairs, Chem. Biol. 13 (5) (2006) 521–530.

[15] N. Heim, O. Griesbeck, Genetically encoded indicators of cellular calcium dynamics based on troponin C and green fluorescent protein, J. Biol. Chem. 279 (14) (2004) 14280–14286.

[16] N. Heim, O. Garaschuk, M.W. Friedrich, M. Mank, R.I. Milos, Y. Kovalchuk, A. Konnerth, O. Griesbeck, Improved calcium imaging in transgenic mice expressing a troponin C-based biosensor, Nat. Methods 4 (2) (2007) 127–129.

[17] M. Mank, D.F. Reiff, N. Heim, M.W. Friedrich, A. Borst, O. Griesbeck, A FRET-based calcium biosensor with fast signal kinetics and high fluorescence change, Biophys. J. 90 (5) (2006) 1790–1796.

[18] M. Mank, A.F. Santos, S. Direnberger, T.D. Mrsic-Flogel, S.B. Hofer, V. Stein, T. Hendel, D.F. Reiff, C. Levelt, A. Borst, T. Bonhoeffer, M. Hübener, O. Griesbeck, A genetically encoded calcium indicator for chronic in vivo two-photon imaging, Nat. Methods 5 (9) (2008) 805–811.

[19] H. Zhao, L. Giver, Z. Shao, J.A. Affholter, F.H. Arnold, Molecular evolution by staggered extension process (StEP) in vitro recombination, Nat. Biotechnol. 16 (3) (1998) 258–261.

[20] M. Ouyang, J. Sun, S. Chien, Y. Wang, Determination of hierarchical relationship of Src and Rac at subcellular locations with FRET biosensors, Proc. Natl. Acad. Sci. USA 105 (38) (2008) 14353–14358.

[21] T. Nagai, S. Yamada, T. Tominaga, M. Ichikawa, A. Miyawaki, Expanded dynamic range of fluorescent indicators for Ca^{2+} by circularly permuted yellow fluorescent proteins, Proc. Natl. Acad. Sci. USA 101 (29) (2004) 10554–10559.

[22] R.S. Lewis, The molecular choreography of a store-operated calcium channel, Nature 446 (7133) (2007) 284–287.